# Acoustic Echo Formation — A Filter Theory Approach

Adam Zielinski, University of Victoria
Department of Electrical and Computer Engineering
P.O. Box 3055
Victoria, BC V8W 3P6 Canada
E-Mail: adam@ece.uvic.ca

Jaroslaw Tegowski, Polish Academy of Sciences
Institute of Oceanology
Ul. Powstancow Warszawy 55
81-712 Sopot, Poland
E-Mail: tegowski@iopan.gda.pl

***Abstract*- The response of a reflecting boundary, such as an ocean bottom, to an impinging acoustic pulse involves several processes and variables. One group of these processes is associated with the formation of an acoustic transmitting/receiving beam and with the parameters of the transmitted acoustic pulse. Another group is associated with the complex physical processes involved in sound reflection and scattering from the surface and the volume of the ocean bottom. The complexities of these phenomena often obscure an intuitive understanding of the underlying principles of echo formation and its reception. In this paper, we propose a simplistic model for this complex process using filter theory. The bottom is represented as a surface reflector with an acoustic wave front sweeping over it with time-varying velocity. The impulse response of a smooth flat bottom is characteristic of a low pass-filter that will greatly attenuate the impinging high frequency pulse. On the other hand, bottom undulations will modulate the reflected signal such that it can be represented by the impulse response of a band-pass filter. The received echo can be represented as the response of such filter to a high frequency probing pulse. The characteristics and amplitude of the echo are dependent on frequency spectrum overlap between the transmitted pulse spectrum and the filter frequency response. In the paper, we discuss several cases of interest with the intent to provide an intuitive understanding of echo formation from a system point of view.**

## I. Introduction

The response of a reflecting boundary, such as an ocean bottom, to an impinging acoustic pulse involves several processes and variables. One group of these processes is associated with the formation of an acoustic transmitting/receiving beam and with the parameters of the transmitted acoustic pulse. Another group is associated with the complex physical processes involved in sound reflection and scattering from the surface and the volume of the ocean bottom. Models describing echo formation have been developed which require extensive computations to generate sample time-domain signals [1,2,3]. Our purpose here is to present a simplistic model that can enhance intuitive understanding of echo formation in certain conditions.

## II. The model

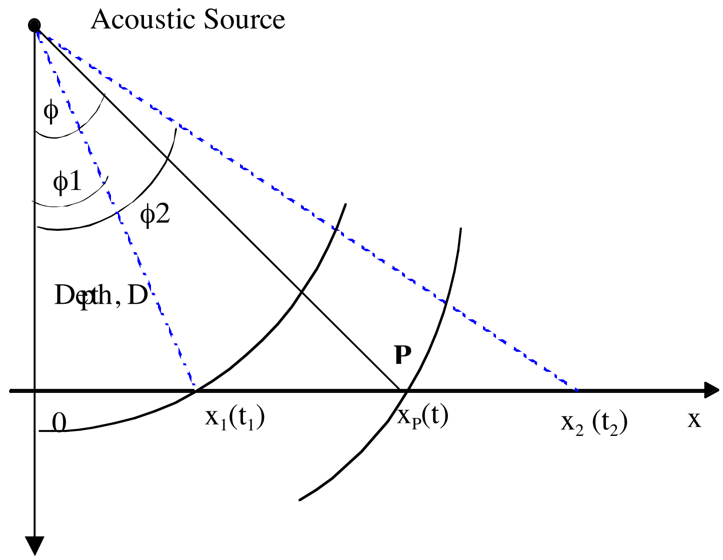


Figure 1. Geometry of the acoustic beam.

The acoustic source is positioned at distance D from a flat horizontal bottom. The same source is used both as a transmitter and as a receiver.

We assume that the acoustic source generates a fan-like beam - narrow in one axis and wide in another, orthogonal axis. The beam is not pointed vertically toward the bottom but is tilted, such as in side-looking sonar, to cover an angular sector ($\phi_1$, $\phi_2$). The footprint of such a beam on a flat bottom can be represented by a narrow strip extending from distance $x_1 = D\tan(\phi_1)$ to $x_2 = D\tan(\phi_2)$ as shown in Figure 1. The spherical wave front originating from the source travels with sound velocity c = 1.5 m/ms and intercepts the bottom at point P which position $x_p(t)$ moves along the x-axis as a function of time, given by (1):

$$x_P(t) = \sqrt{(D + ct)^2 - D^2}\,. \qquad (1)$$

We choose the time origin t = 0 as the time when the spherical wave front intercepts the bottom first at point x(0) = 0.

The velocity v(x) of this moving point P(x) is a function of its position x on the x-axis:

$$v(x) = c\sqrt{\left(\frac{D}{x}\right)^2 + 1} \qquad (2)$$

or, as a function of time:

$$v(t) = c\frac{D + ct}{\sqrt{ct(2D + ct)}}. \qquad (3)$$

Figure 2 shows position of point P, $x_P(t)$ and its velocity v(t) for different bottom depths D: 100m, 200m, 300m, 400m and 500m.

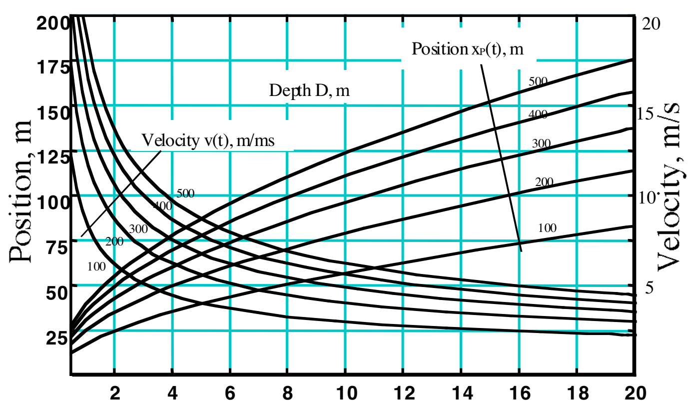

Figure 2. Position and velocity of intercept point P.

We note that the velocity is infinite at x = 0 and then approaches sound velocity for x >> D. A point P on axis x, P(x) = P(ϕ) will be reached after a certain delay τ(x) associated with additional travel distance. That is:

$$\tau(x) = \frac{\left(\sqrt{D^2 + x^2} - \sqrt{D^2}\right)}{c} = \frac{D(1 - \cos(\phi))}{c\cos(\phi)}. \qquad (3)$$

The average velocity of the point P traveling over the $(x_2\text{-}x_1)$ distance is given by:

$$v_{av} = \frac{x_2 - x_1}{t_2 - t_1}. \qquad (4)$$

Table I lists sample numerical values for depth D = 200 m and a beam width Ω = $20^o$ pointing at $15^o$ +/- $10^o$ and, therefore, covering an angular sector from $\phi_1 = 5^o$ to $\phi_2 = 25^o$.

Table 1. Sample values

| **t, ms** | **$x_P$(t), m** | **v(t), m/ms** | **$v_{av}$, m/ms** |
|---|---|---|---|
| t = $t_1$ = 0.51 | $x_1$=17.5 | $v_1$=17.2 | 5.71 |
| t= $t_2$ = 13.78 | $x_2$=93.3 | $v_2$=3.55 | 5.71 |

**III. Transmitted acoustic probing pulse**

Assume a base-band pulse A(t) > 0 with a certain effective duration $\tau_p$. Its spectrum extends from zero frequency and has a spectral width (bandwidth) given approximately by:

$$B = 1/\tau_p. \qquad (5)$$

This pulse can be used to amplitude modulate a carrier wave with frequency f. The resulting pulse is called a HF pulse. A transmitted HP pulse s(t) can be represented in complex notation **s(t)** (phasor notation) as:

**s**(t) = A(t) exp(j2πft) (6)

such that

s(t)=Re{**s**(t)}. (7)

The spectrum of a HF pulse is centered around the carrier frequency and has bandwidth:

$$B_{HF} = 2B. \qquad (8)$$

As the carrier frequency f is lowered, the spectrum of the pulse moves to baseband (lower) frequencies.

**IV. Echo formation**

The reflected echo **e**(t) signal in complex notation is obtained by integration of the bottom returns over the beam footprint:

$$\mathbf{e}(t) = \exp(j2\pi ft)\int_{x1}^{x2} B(x)A(t - \tau(x))\exp(-j2\pi f\tau(x))dx \qquad (9)$$

where B(x) is a function related to the width of the beam footprint at the bottom, the bottom reflection coefficient at a certain incident angle and the two-way beam pattern.

The echo envelope is:

Env(t) = |**e**(t)| . (10)

**IV. Flat bottom impulse response**

Suppose that the transmitted pulse is an idealized, infinitely short delta-pulse that travels over the flat bottom. Each intercepted point generates an echo traveling towards the transmitter, resulting in a continuous bottom response called the impulse response $h_B(t)$. For an ideally smooth bottom, $h_B(t) = 0$. Here, we assume that the botttom is flat but not perfectly smooth and therefore $h_B(t)$ is small but not zero. Let us denote by $\tau_{max}$ tthe effective duration of such a response equal the double maximum echo time spread associated with beam coverage (two-way travel time from and back to the source). The bottom impulse response can be modeled by the impulse response of a low-pass filter with bandwidth

$$B_B = 1/\tau_{max}. \quad (11)$$

The echo reflected from a flat bottom s(t) can be considered as a response of such a low-pass filter to a HF probing pulse as given by (7). It can be calculated in time domain by convolution:

$$e(t)=s(t)\otimes h_B(t) = h_B(t)\otimes s(t) \quad (12)$$

where $\otimes$ denotes convolution operation.

The echo spectrum can be presented in the frequency domain as:

$$E(j\omega) = S(j\omega)H_B(j\omega) \quad (13)$$

where $S(j\omega)$ and $H_B(j\omega)$ are Fourier transforms of s(t) and $h_B(t)$ respectively. The echo amplitude and shape will depend on the extent to which the spectra $S(j\omega)$ and $H_B(j\omega)$ overlap and interact with each other. Since $H_B(j\omega)$ represents a frequency response of a low-pass filter, the echo from a smooth flat bottom will, therefore, be more pronounced for:

- the lower spectrum of the transmitted probing pulse, that is, for the lower carrier frequency of the probing pulse. Ideally the probing pulse should be a base-band pulse.
- a narrower bottom coverage obtained by a narrow beam that generates a shorter bottom impulse response and, therefore, a wider bandwidth extending towards probing pulse frequency band.

We will illustrate these points by considering parameters as given in Table 1 for which $\tau_{max} = 2(t_2-t_1) =$ 26.5ms. The flat bottom low-pass filter has, therefore, a bandwidth $B_F = 1/\tau_{max} = 37.7$ Hz. The impulse response of such a low-pass filter was modeled by double real poles at 20 Hz and is shown in Figure 3. This impulse response has a finite rise time with gradual decay and effective duration of approximately 26ms. It models well the actual situation considering a non-uniform shape of an acoustic beam. We assume a rectangular probing pulse of duration 1ms. Figure 4a shows the filter response (echo) to a probing rectangular pulse with one carrier cycle in the pulse while Figure 4b shows the response for 3 carrier cycles in the pulse. The filter gain was set to 40dB for each case.

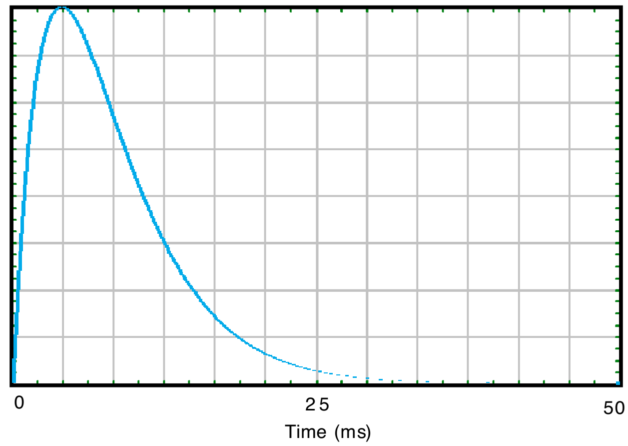


Figure 3. Impulse response of a flat bottom.

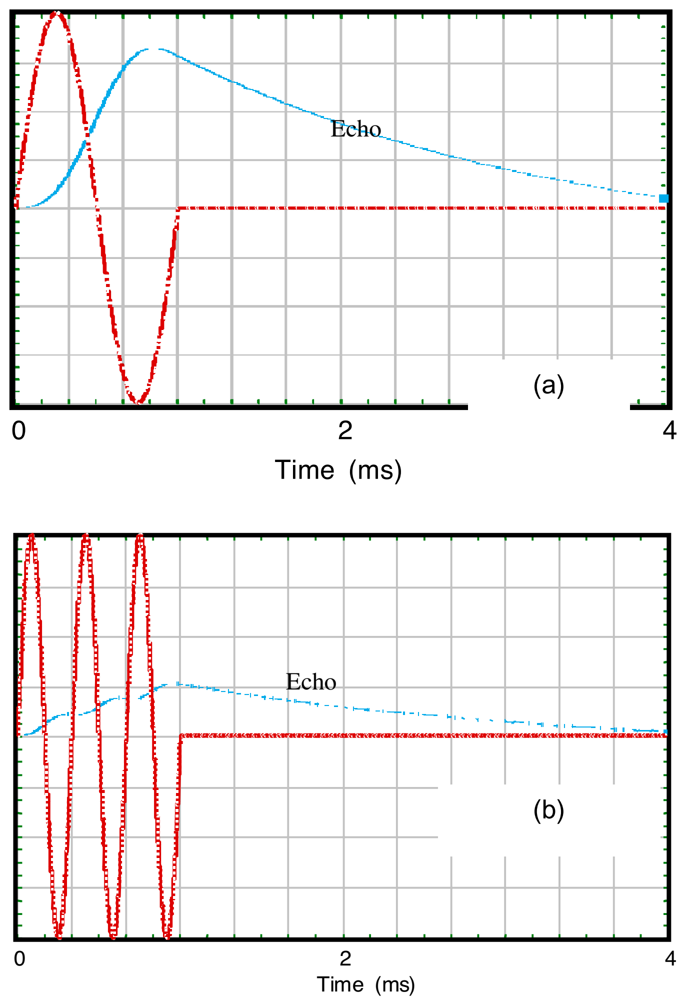


Figure 4. Echo formation from a flat bottom.

We observe, as expected, a rapid decrease in its amplitude for the increased carrier frequency of the pulse (number of cycles within the pulse).

**V. Non-uniform bottom**

The actual bottom has in general a non-uniform random surface with certain statistical properties. Such a surface will modulate the impulse response of the bottom. The exact nature of this modulation is a complex process that can be related to the bottom reflection coefficient and the incident angle at each point of the reflecting surface. For simplicity, we assume that modulating bottom undulations are sinusoidal with a spatial period T. We also make the important assumption that the wavefront intecepts the bottom for a given t only at one point P. To satisfy this assumption the minimum incident angle $\phi_{min}$ must be larger than 90° minus the angle of maximum bottom slope. The impulse response of such a bottom can be modeled as generated by a traveling point $x_P(t)$ along such a bottom with the time-varying velocity v(t) as given by (2) or (3), that is:

$$h_{HF}(t) = B(t) \sin [2 \pi f(t)t] \quad \text{for } t_1 < t < t_2 \qquad (14)$$

and 0 otherwise

where instantaneous frequency f(t) is related to spatial period T and point P velocity v(t) as:

$$f(t) = v(t)/T \qquad (15)$$

and function $B(t) > 0$ is an envelope of the bottom impulse response.

Such an impulse response is a chirp signal with instantaneous frequency being a nonlinear function of time. Using values as in Table 1 and assuming bottom undulations with spatial period T= 0.1m we see that the instantaneous frequency of the impulse response for the duration of the pulse will vary from $f(t_1)$ = 172 kHz to $f(t_2)$ = 35.5 kHz. For a very large $t_2$, the frequency will stabilize at $f(\infty) = c/T$ = 15 kHz. As in the flat-bottom case, the character and the amplitude of the bottom response to the HF pulse will depend on the frequency overlap of the HP pulse and the bottom impulse response spectra. To illustrate this point, we will use values from Table 1 but for simplicity we will assume a constant instantaneous frequency of bottom impulse response equal to average velocity $v_{av}$ as given

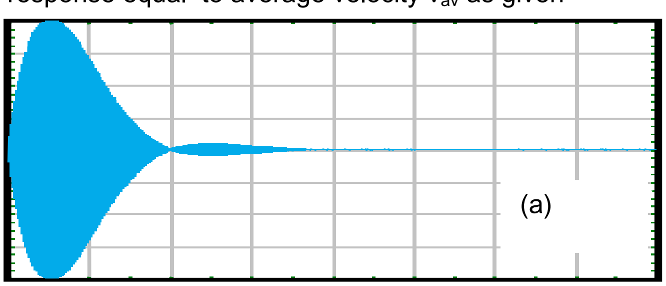


by (4). Using (15), we find that this frequency is 57 kHz. We model such response as an impulse response of a resonant narrow filter with resonant frequency at 57 kHz with impulse response shown in Figure 5a.

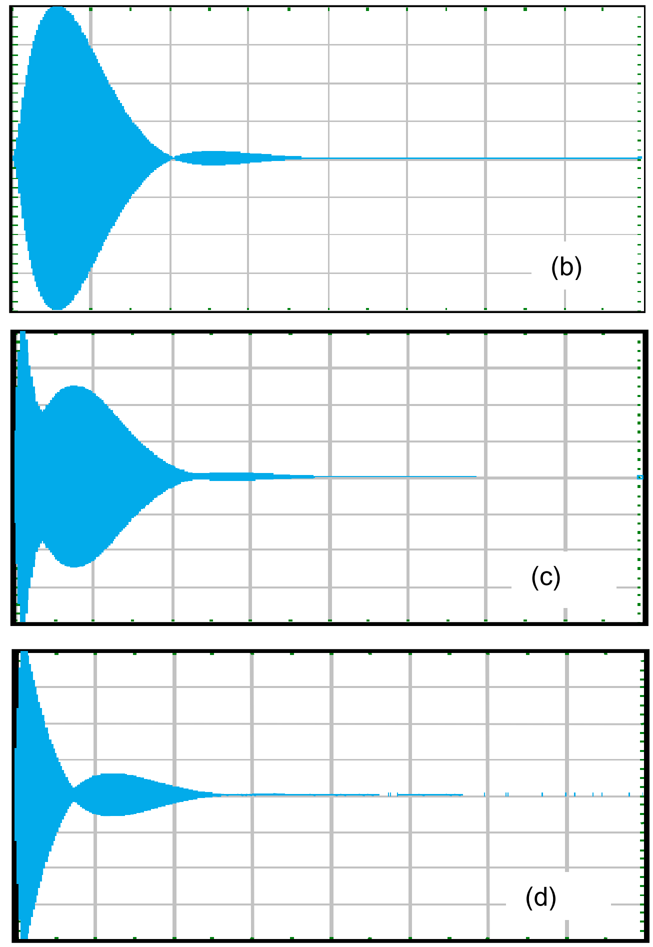


Figure 5. Time domain responses all on time scale of 100ms and normalized peak amplitudes (a) Impulse response of the bottom filter of 57 kHz (b) Response to matched probing pulse of 57 kHz (c) Response to mismatched pulse of 47 kHz (d) Response to mismatched pulse of 67 kHz

The effective duration of the filter response is approximately 25ms. Figure 5b shows the echo for a rectangular probing pulse of 1ms duration with the same (matched) central frequency as the bottom filter, that is, 57 kHz. Figure 5c and 5d show effects of frequency mismatch that demonstrated itself by the change of the echo shape and drastic drop in their amplitudes that were reduced to 0.5% of the matched pulse case.

**VI. Chirping bottom response**

For more accurate and realistic results, we also consider a bottom with a chirp response. Since the spectrum of such impulse has a broader frequency band, we expect less sensitivity to the mismatched probing pulse frequency. We use again the situation shown in Table 1 and T = 0.1m. The instantaneous frequency of the bottom response as given by (15) for two way travel time can be approximated by:

$$f(t) = \frac{72.29}{0.5t + t_1} + 30.25 \qquad (16)$$

where f is in kHz and t is in ms and $t_1 = 0.51$.

Since the order of the convolution operation is optional as indicated by (12) we can conveniently reverse the role of probing pulse with the impulse response of the bottom. After such a change of roles, the transmitted probing pulse will have a relatively long duration (with the envelope as shown in Figure 3) and time-varying carrier has instantaneous frequency varying according to (16). This chirping frequency changes from f(0) = 141.7 kHz to $f(t=t_2-t_1=13.27) = 40.2$ kHz. The bottom response is now modeled by a response of a fixed resonant filter with a narrow bandwidth, a fixed central frequency 40.2 kHz < $f_o$ < 141.7 kHz and short duration of impulse response of approximately 1ms. Such a filter will respond to the input chirp signal with high output at the time the input frequency passes through $f_o$. Varying $f_o$ will not only affect the shape and amplitude of the filter response but also its delay. We illustrate this effect by responses of two narrowband filters centered at 100 kHz and 50 kHz respectively to a chirp input signal as shown in Figure 6.

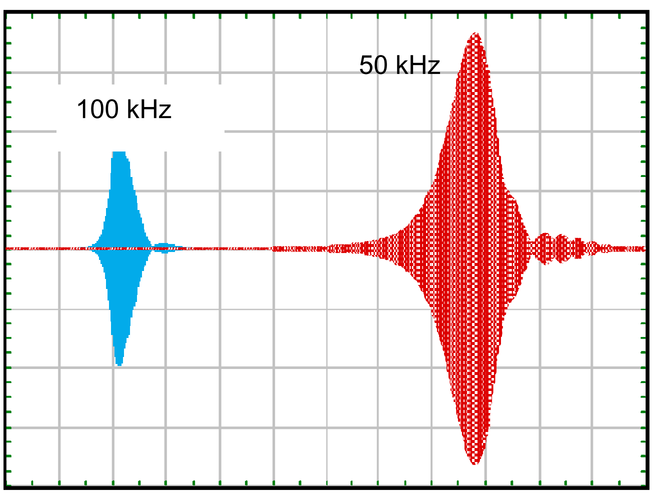


Figure 6. Response for two different probing pulses.

The chirping signal will excite first the 100 kHz-filter before the 50 kHz-filter. The sweeping speed is faster for higher frequencies; therefore, the 50 kHz-filter generates a broader and higher amplitude pulse at its output. This effect indicates the different performance of the actual sonar system depending on the frequency of the probing pulse.

**VII. Future work**

Future work will include a bottom model as a random surface as well as generalization to two-dimensional beams.

**References**


[1] Michael H. Brill, Xavier Zabal, and Stanley L. Adams, "Time spread of acoustic signals reflecting from a fixed rough boundary," J. Acoust. Soc. vol.74 (4), pp. 1063- 1070, 1984.

[2] E. Pouliquen, O. Bergem, and N. G. Pace, "Time-evolution modeling of seafloor scatter. I. Concept," J. Acoust. Soc. Am. 105 (6), pp. 3136—3141, 1999.

[3] O. Bergem, E. Pouliquen, G. Canepa, and N. G. Pace, "Time-evolution modeling of seafloor scatter. II. Numerical and Experimental Evaluation," J. Acoust. Soc. Am. 105 (6), pp. 3142- 3150, 1999.